Heliyon 8 (2022) e10245

Contents lists available at ScienceDirect

Heliyon

journal homepage: www.cell.com/heliyon

Research article

Groundwater potential zonation using VES and GIS techniques: A case study of Weserbi Guto catchment in Sululta, Oromia, Ethiopia

Desalegn Dhinsa [b], Fekadu Tamiru [a], Birhanu Tadesa [a,*]

[a] Department of Earth Science, Wollega University, Nakamte, Ethiopia
[b] School of General Tadesa Birru, Finfine, Ethiopia

ARTICLE INFO

Keywords:
Geographic information system (GIS)
Geoelectrical
Multi-criteria evaluation (MCE)
Apparent resistivity
Pseudo cross-section

ABSTRACT

Groundwater is an appreciated and vital natural resource in the world, and it is of the utmost essential for the growth and development of a country. Nevertheless, assessing the groundwater potential and its recharge region is still ambiguous due to the nature of groundwater. In this study, the groundwater potential of the Weserbi Guto Laga Qawe Catchment Sululta area was assessed using VES and GIS methods. For the model, thematic layers were generated from the geophysical investigation, existing maps, and field survey results and were integrated into the GIS environment to delineate the groundwater potential zones. Factors such as lineament density, drainage density, elevation or topography, slope gradient, aquifer resistivity, and lithology were derived, reclassified, and scaled to common ranges and assigned with appropriate weights. The groundwater potential zonation model of the site was produced by the multicriteria evaluation method. Accordingly, the geometrical interval method was utilized to classify the index into three zones (high, moderate, and low) to produce the map. The model result revealed that a large part of the study area fell into the high zone with 50.14 % (3669.99ha). whereas 35.85% (262.72ha) and 14.01% (1024.95ha) show moderate and low groundwater potential, respectively. The resulting map was validated using eleven existing water level data points and the result was found to be in good agreement with the model.

1. Introduction

Water is one of the fundamental natural resources for all living things to exist on the earth, and it plays a vital role in bringing significant socio-economic development. It is essential to the existence of humans and all living things. Groundwater occurs almost everywhere beneath the earth's surface, not only in a single widespread aquifer but also in thousands of local aquifer systems. It is the safest and most reliable source of water for domestic, irrigation, industry, and municipal purposes. It is the portion of atmospheric precipitation that has percolated into the earth to form a groundwater occurrence. Worldwide, more than 1 billion people lack access to safe drinking water (USDA, 1986). As USDA (1986) noted, 67% of the rural populations in developing countries are affected by the scarcity of water. As Rosen and Vincent (1999) point out, they are not all harmless water sources as a supply. People living in rural areas, particularly in developing countries, will rely on surface water for sustenance and survival.

Water supply rates in Ethiopia were extremely low, at 19% of national averages, and 11.5% in agricultural villages (based on data collected in 1990–1991), compared to 41% of Sub-Saharan African averages (Jiaca, 2002). The uneven distribution of groundwater from one space to another is part of a problem in hydrology. This, in turn, affects the depth of the groundwater table on the different geologic horizons. So, it is very important to delineate areas of low resistivity due to effects associated with permeability and structure of the geological formation and the amount of water-bearing capacity.

The groundwater potential of the Abbey Basin was investigated by the Ministry of Water Resources using geophysical and hydrogeological techniques by water design supervisors. However, the groundwater potential zone in the Weserbi Guto area has not yet been investigated using GIS technology so far. Thus, there is no insufficient spatial information to indicate the location of the groundwater potential zone in the area.

Therefore, this study was focused on mapping the groundwater potential zones for Weserbi Guto Village by an integrated approach of Vertical Electrical Sounding (VES) and Geographical Information System (GIS) techniques. As Sudhakar et al. (2018) found, electrical investigations, mostly VES, were directed to determine the availability of groundwater potential and help locate possible borehole sites for

* Corresponding author.
E-mail address: biretedosa@yahoo.com (B. Tadesa).

https://doi.org/10.1016/j.heliyon.2022.e10245
Received 26 January 2022; Received in revised form 18 April 2022; Accepted 5 August 2022

groundwater extraction. For this reason, it is important to apply proper modeling techniques to characterize the village's groundwater potential.

2. Study area

The Weserbi Guto catchment is located in the Sululta District within the Oromia Regional State, Ethiopia. Sululta is bordered on the south by Finfinnee city, on the west by the Mulo and West Shewa Zones, on the north by the North Shewa Zone, and on the east by Bereh. Weserbi Guto catchment, geographically positioned between latitude 9°4′30″N to 9°10′30″N and longitude 38°39′0″E to 38°46′30″E. and its elevation ranges from 2584m to 3075m above m.s.l (Figure 1). According to the Ethiopian geomorphologic database, residual and volcanic landforms were found in the study area (Figure 2). Likewise, there are six types of geological formations, Cheleka basalt, trachytes, Entoto volcanic, middle basalts, quaternary basalts, and quaternary superficial sediments (Figure 3).

3. Materials and methods

In this study, primary and secondary data were used. These data sets include Digital Elevation Model (DEM) results from (https://search.asf.alaska.edu/#/), Waterpoint inventories, and VES data interpretation results from a field survey. Those data were used to model groundwater potential in the study area (Table 1).

3.1. VES method

The VES geophysical technique was used to acquire the aquifer resistivity layer parameters with different lithological formations. VES (Schlumberger sounding) is well applied for groundwater searches because of its simplicity and propriety (Venkateshwara et al., 2014). Twenty-five VES data points were collected using the Syscal Junior Switch 72 (IRIS) instrument with a Schlumberger array along with five profiles within the Weserbi Guto catchment (Figure 1). Electrodes are used in series to detect the variation of resistivity in depth. The instrument was adjusted to measure the possible readings in 2 s to give the average value of apparent resistivity for every set of current and potential electrode separations. The VES data was conducted with half current electrode spacing of 500m and maximum potential electrode spacing of 90m. Analysis of VES data provides reliable information related to distinct geological formations, landforms, and drainages that are essential in groundwater exploration. The resistivity and thickness parameters were determined using the Ip2Win (http://geophys.geol.msu.ru/demo_exe/SetUp_lt.exe) computer program applications. The number of layers assigned is based on the bends of the graph created by connecting the points created by resistivity values on the y-axis versus AB/2 on the x-axis.

3.2. GIS method

According to Çelik, (2019), GIS-based multicriteria decision making (MCDM) is an admirable evaluation method that evaluates different criteria procedures in GIS. The investigation procedure was executed by different QGIS tools (https://qgis.org/en/site/forusers/download.html#) that were used to grade and interpolate the thematic factors. The groundwater potential model (GPM) was produced by a collection of parameters that depict the normal events of groundwater. To model the groundwater potential zone inside the catchment, topical layers of geology (lithology), slant slope, aquifer resistivity, elevation/topography, lineament density, and drainage density were organized within the GIS environment. These datasets are evaluated and weighted to account for the contribution of groundwater occurrence. Figure 4 shows the stages of the methodological preparation of the thesis.

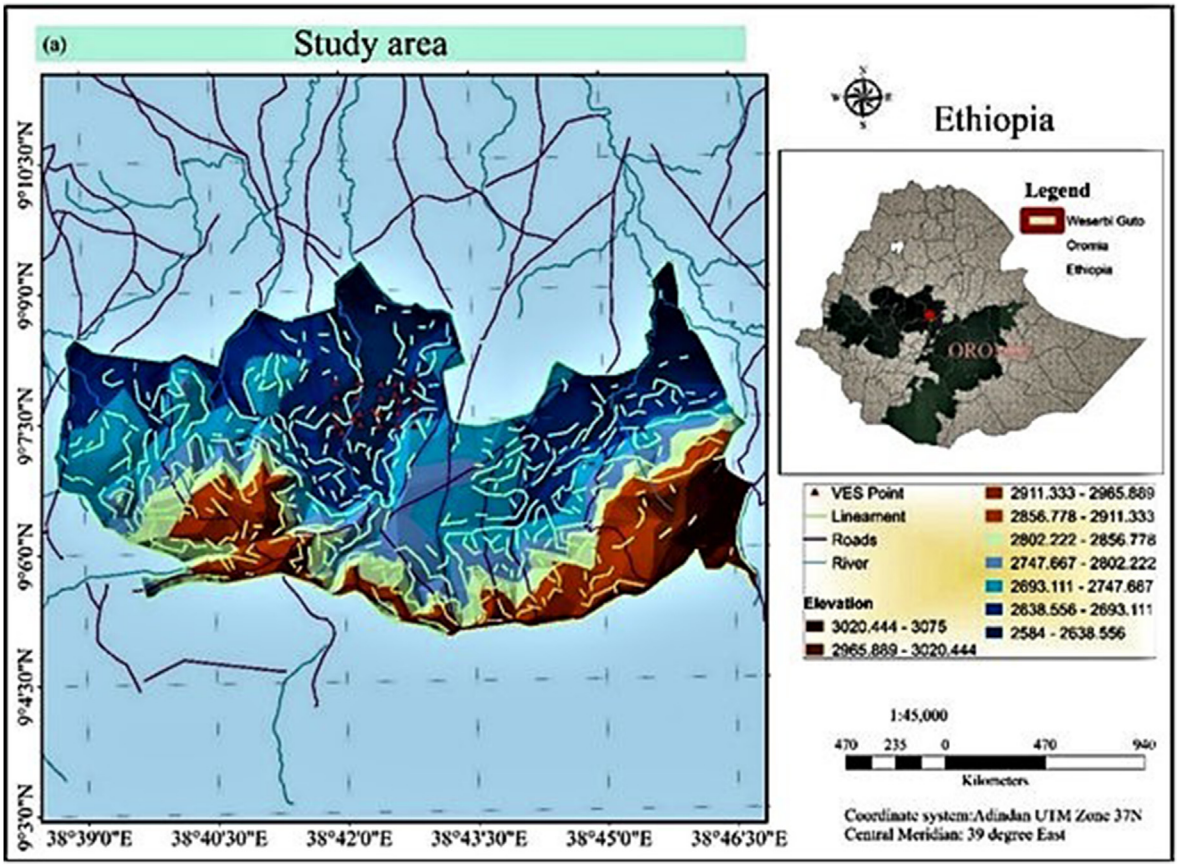

Figure 1. Map of the study area (Weserbi Guto).

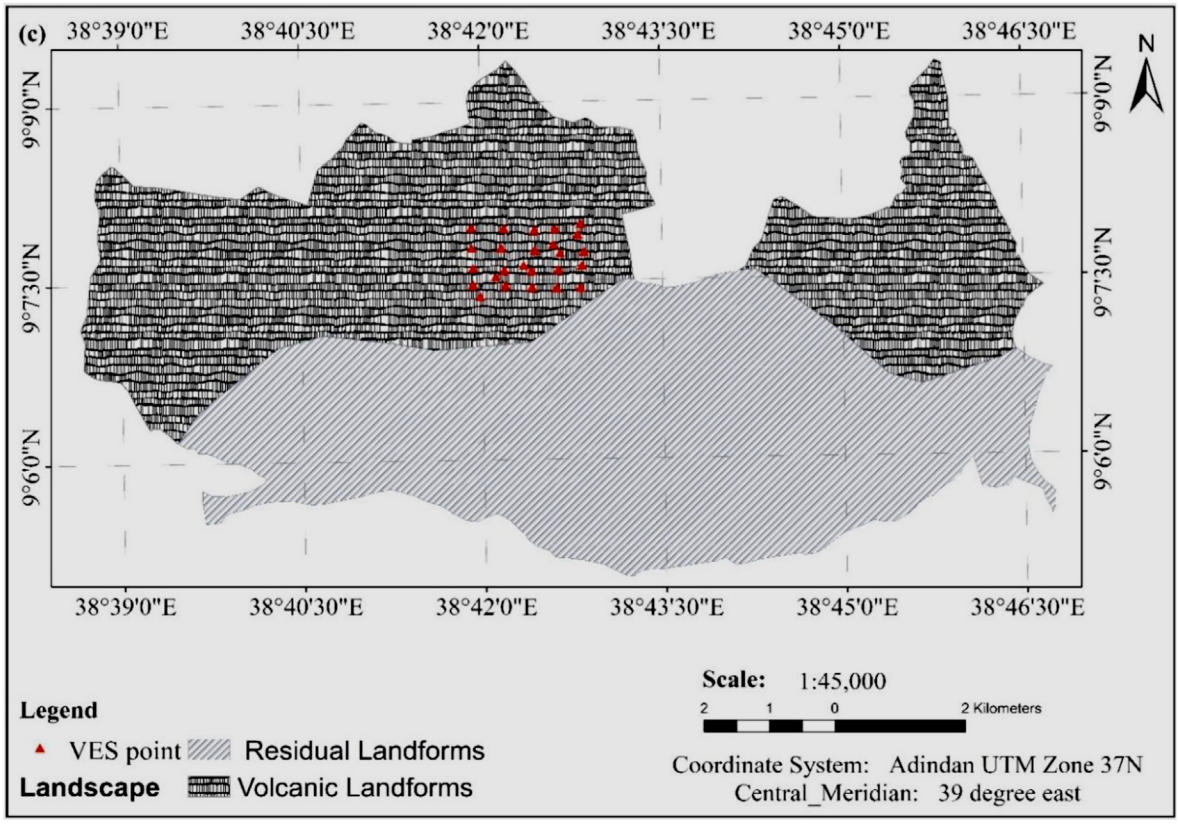

Figure 2. Geomorphical map of Weserbi Guto

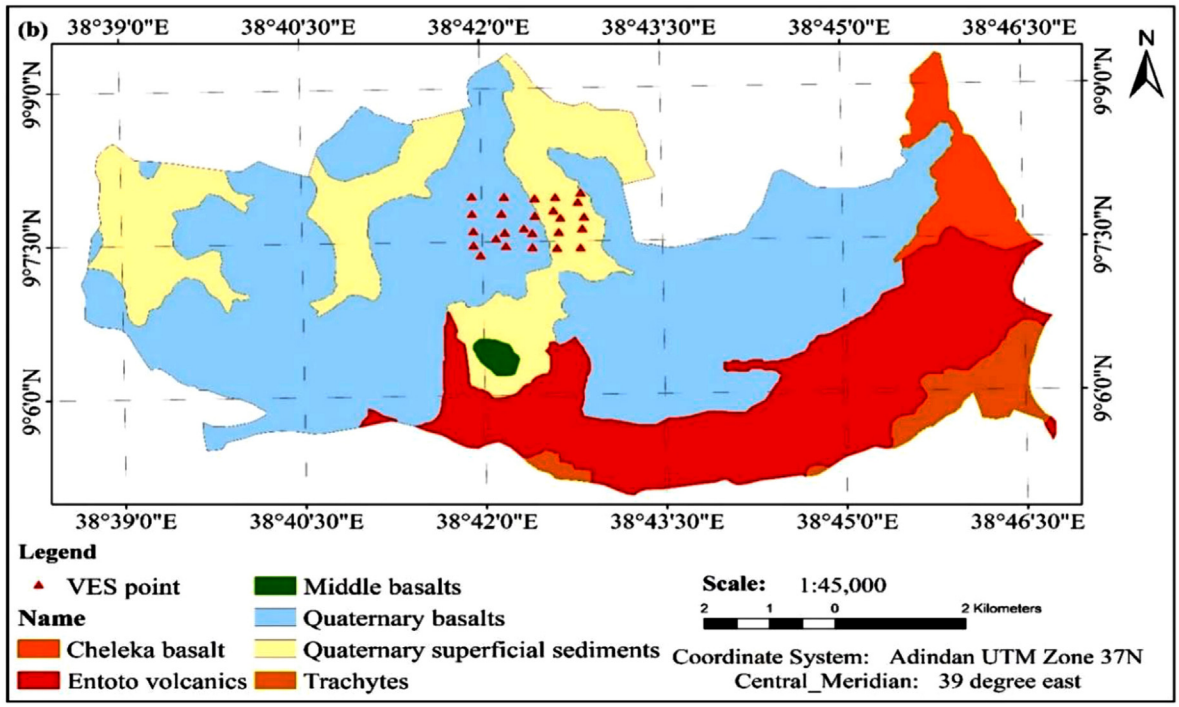

Figure 3. Geological map of the study area.

4. Results and discussion

4.1. Resistivity interpretation

The interpretation of VES resistivity point data along all profiles has been presented in this section.

4.1.1. Curve interpretation along profile one

The results of the VES points of profile one (P1V1, P1V2, P1V3, P1V4, and P1V5) showed a five to six-layer model of resistivity (Figure 5). P1V1curve represents $\rho_1 > \rho_2 > \rho_3 > \rho_{4<}\rho_5$. In the overall inversion, the RMS error was 2.22%, which was achieved after the iterations. The lithologies under the VES point P1V2 were categorized into five layers and

Table 1. Types of data and data source.

Data Types	Data	Resolution/Format	Source	Functions
Primary Data	DEM Data	12.5m	ASFDAAC	Utilized to form Slant slope, Geology, lineament, and waste
	VES Data	Excel format	Geoelectrical Surveying	Used to produce aquifer resistivity and lithology factors
Secondary Data	Borehole Data	Excel Format (1998–2003)	Handled GPS	Used to validate the groundwater potential map
	Soil texture	Shape File	Ministry of Agriculture	Collected soil factor
	Geomorphology	Shapefile	Geological Survey of Ethiopia	Used to map Geomorphology of the study area
	Rainfall	Excel format	Ethiopian Metrological Agency	generated rainfall factor
	Boundary	Shapefile	Ethiopia Geospatial Agency	To portray location map and zonal information

the curve represents $\rho_1 > \rho_2 < \rho_3 < \rho_4 > \rho_5$; Whereas the P1V3 curve is represented as $\rho_1 > \rho_2 > \rho_3 < \rho_4 > \rho_5$. This type of layer is a QK-type layer, and it has five layers. P1V4 classifies the possible litho-logic formation into five layers, and the curve represents $\rho_1 < \rho_2 < \rho_3 < \rho_4 > \rho_5$ with AK- type curve. The VEs point P1V5 curve represents $\rho_1 > \rho_2 > \rho_3 < \rho_4 > \rho_5 > \rho_6$ a QQ-type layer and the curve has six layers.

4.1.2. *Pseudo cross-section along profile one*

The VES data along all survey lines were used to construct the pseudo section to identify the distribution of different resistivity values in the lateral and vertical directions. Pseudo-depth maps were produced from apparent resistivity data and show both the general lateral and vertical resistivity variation in the subsurface. The pseudo section prepared from all VES that lie on the line of profile one was determined as shown in Figure 6 below. The pseudo-depth section along profile 1 (Figure 6) indicates that the topmost part has a low apparent resistivity value. This is likely to be the response of top-dry soil composed of different-sized sediments derived from weathering of the underlying rock materials. The lower part indicates relatively high resistivity, which signifies a weathered geological formation filled with groundwater.

4.1.3. *Curve interpretation along with profile two*

As observed in Figure 7, the results for the VES points of profile two (P2V1, P2V2, P2V3, P2V4, and P2V5) indicated a five to six-layer model of resistivity. P2V1 divides possible litho-logic division into five layers, and the curve represents $\rho_1 > \rho_2 < \rho_3 < \rho_4 > \rho_5$. This type of curve is an

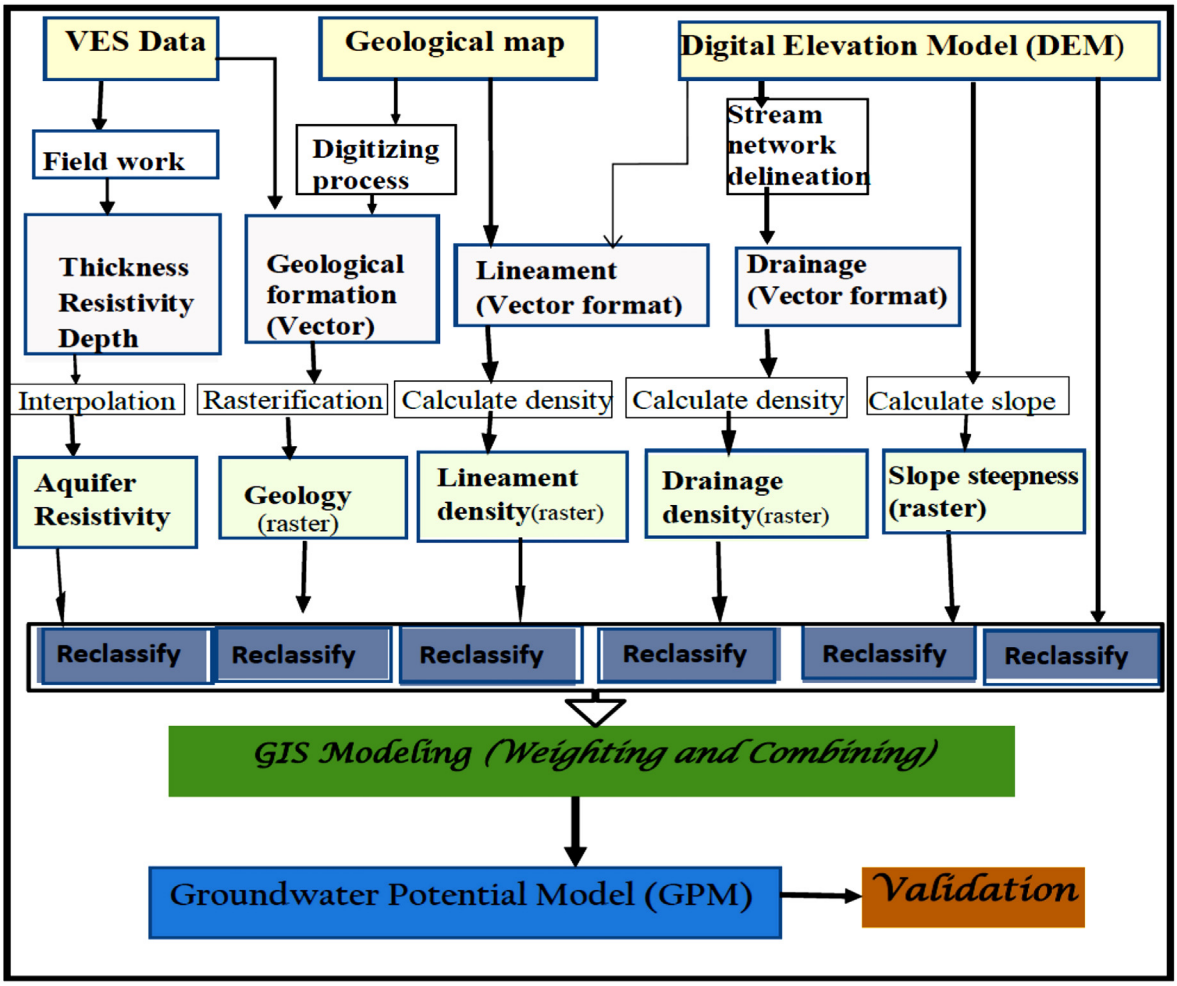

Figure 4. Workflow of Groundwater potential model of study area.

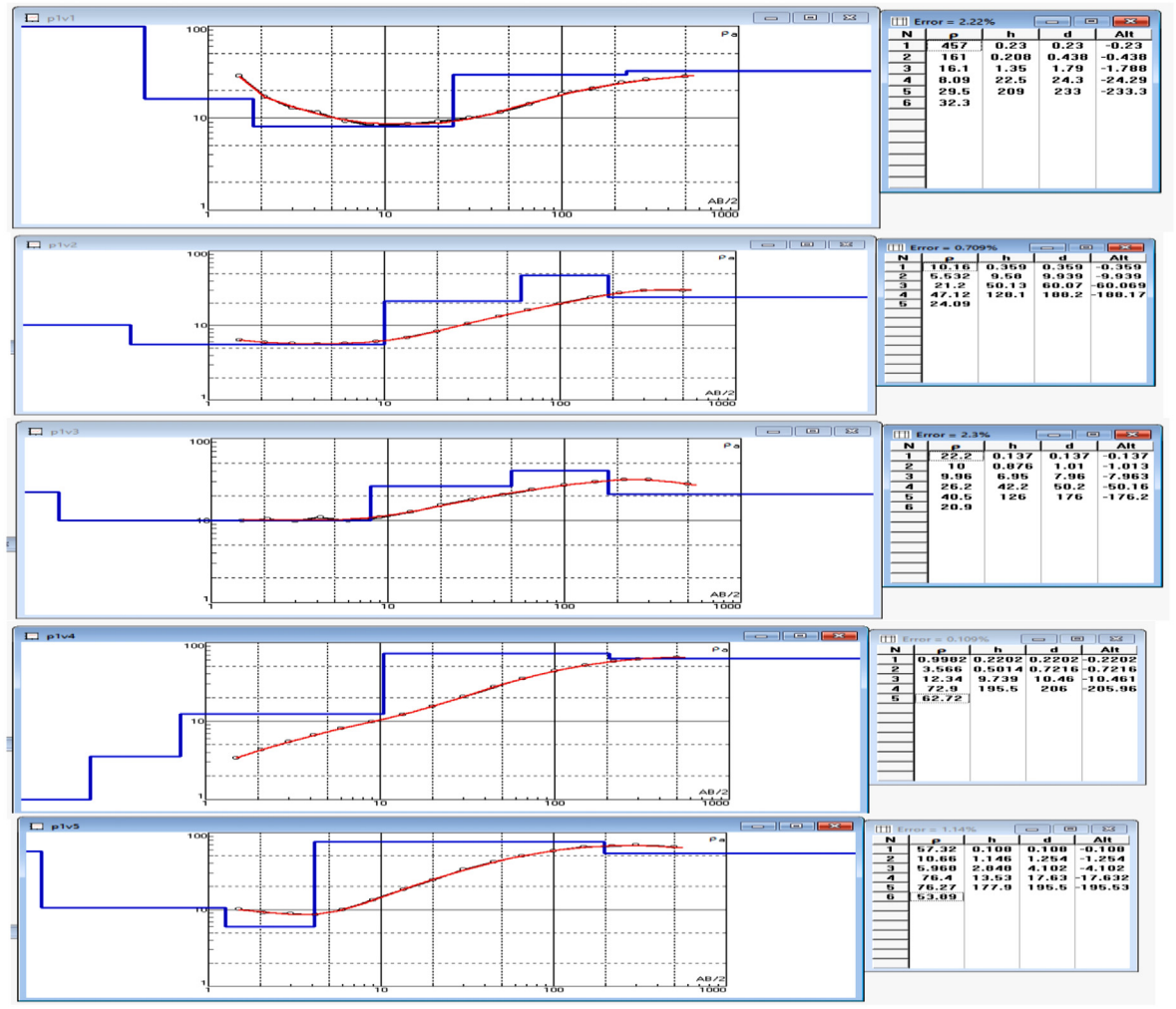

Figure 5. Resistivity sounding curves for Profile one.

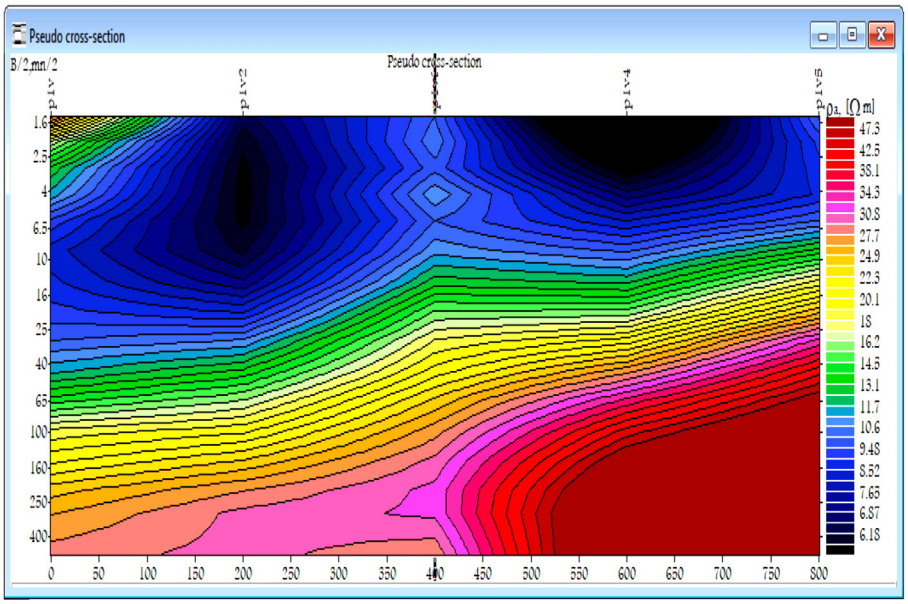

Figure 6. Apparent resistivity pseudo cross section for profile 1.

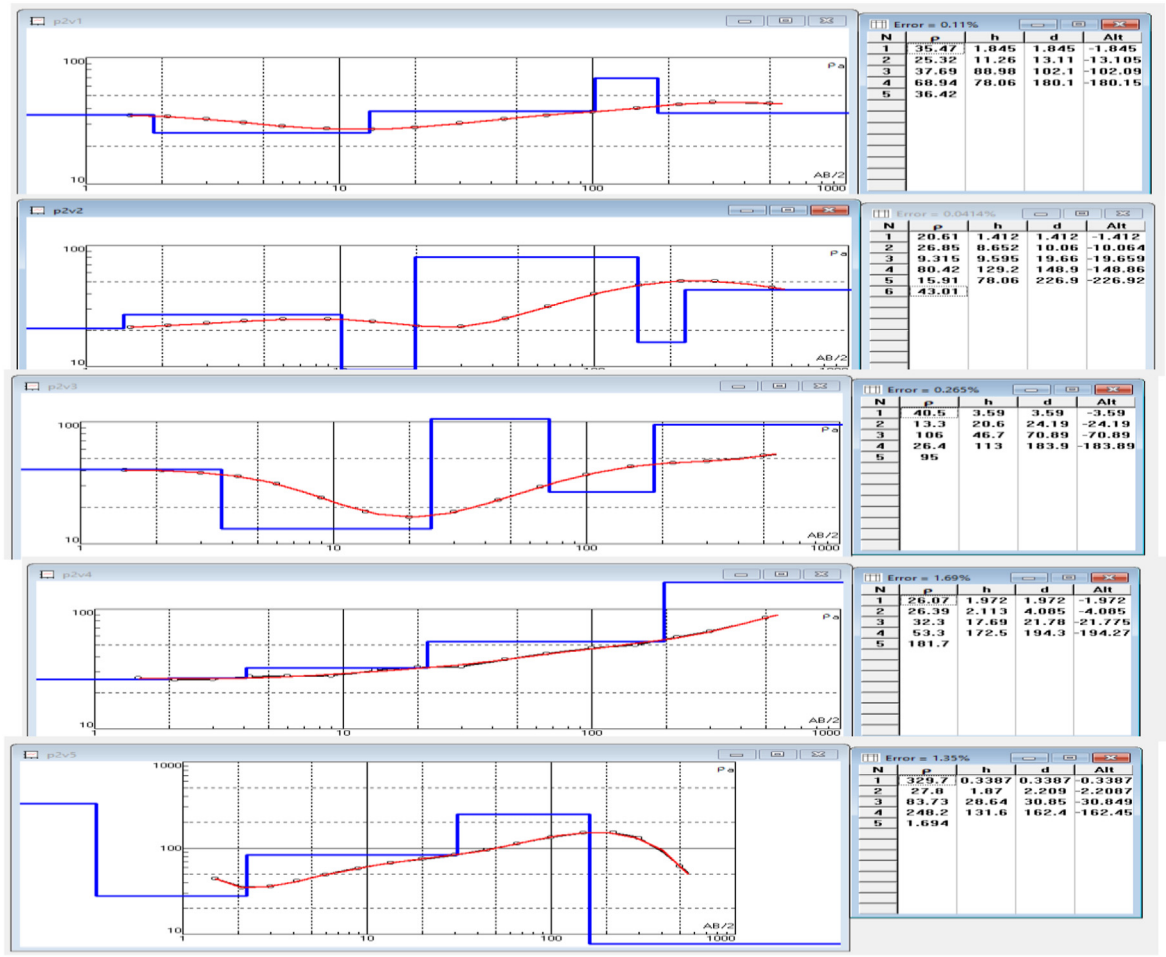

Figure 7. Resistivity sounding curves for Profile Two.

HK-type layer. P2V2 has six layers, and the curve represents $\rho_1 < \rho_2 > \rho_3 < \rho_{4>}\rho_5$, this type of curve was an HH-type layer. P2V3 the curve represents$\rho_1 > \rho_2 < \rho_3 > \rho_4$. This type of layer was the HK-type layer, and the curve had five layers. P2V4 divides the possible litho-logic formation into five layers. The curve represents $\rho_1 < \rho_2 < \rho_3 < \rho_4$ and the type of layer was an AA-type layer. P2V5 has five layers, and the curve represents $\rho_1 > \rho_2 < \rho_3 < \rho_{4>}\rho_5$, this type of curve was an HK-type layer.

4.1.4. Pseudo cross-section along with profile two

As shown in Figure 8, the apparent resistivity along Profile-2 consists of P2V1, P2V2, P2V3, P2V4, and P2V5 points oriented in an NW- SE direction. The pseudo-depth section along with profile 2 (Figure 5) shows four distinct regions. The topmost layers have a relatively low apparent resistivity value, and this is likely to be the response of the less compacted, relatively dry soil materials derived from the in-situ breakdown of the underlying rock materials. It was shown that there was a lateral variation in resistivity value at the bottom and top parts. The lower portion and the southeast portion have relatively high resistivity values.

4.1.5. Curve interpretation along with profile three

As observed in Figure 9, the results for the VES points of profile three (P3V1, P3V2, P3V3, P3V4, and P3V5) gave five to six-layer models of resistivity. P3V1 curve represents $\rho_1 > \rho_{2<}\rho_3 < \rho_{4>}\rho_5$. This type of layer was the HK type layer and the curve had five layers. P3V2 curve represents $\rho_1 > \rho_2 < \rho_3 > \rho_{4<}\rho_5$, this type of layer was an HH-type layer, and the curve had five layers. P3V3 curve represents $\rho_1 < \rho_2 < \rho_3 > \rho_{4<}\rho_{5>}\rho_6$. This type of layer was an AH-type layer, and the curve had six layers. P3V4 had five layers and the curve represents $\rho_1 < \rho_2 < \rho_3 > \rho_{4>}\rho_{5<}\rho_6$. This type of layer was an AQ type layer. P3V5 curve represents $\rho_1 < \rho_2 < \rho_3 > \rho_{4>}\rho_{5<}\rho_6$. This type of layer was the AQ type layer, and the curve had five layers.

4.1.6. Pseudo cross-section along with profile three

Figure 10 shows the pseudo depth section for profile three that contains five VES points. From this pseudo section, there is high resistivity in the middle and south parts of the area. The other part of the area was covered by low resistivity in the northern part, especially in the northwest and northeast.

4.1.7. Curve interpretation along with profile four

As observed in Figure 11, the results for the VES points of profile four (P4V1, P4V2, P4V3, P4V4and P4V5) gave five to six-layer models of resistivity. P4V1 divides litho-logic formation into five layers, and its curve represents $\rho_1 > \rho_2 < \rho_{3>}\rho_{4<}\rho_5$. This type of layer was the HH type layer. P4V2 classifies the litho-logic formation into six stratums. Its curve represents $\rho_1 > \rho_2 < \rho_3 > \rho_{4<}\rho_{5<}\rho_6$ and this type of layer was the HH type layer. P4V3 curve represents $\rho_1 < \rho_2 < \rho_3 > \rho_{4<}\rho_{5<}\rho_6$, this type of layer was an AH type layer and has four layers. The P4V4 divides the litho-logic layer into five horizons, its curve represents $\rho_1 > \rho_2 > \rho_{3<}\rho_{4<}\rho_5$ and this type of layer was the AQ type layer. P4V5 divides litho-logic formation into five layers, and its curve represents $\rho_1 < \rho_2 < \rho_{3>}\rho_{4<}\rho_5$. This type of layer was an AH type layer.

4.1.8. Pseudo cross-section along with profile four

The pseudo-depth section constructed for P4V1, P4V2, P4V3, P4V4and P4V5 that lie on the survey profile line-4 was given in Figure 12. According to this figure, relatively high resistivity values are observed in the section's southwest, eastern, and P4V3 regions. The

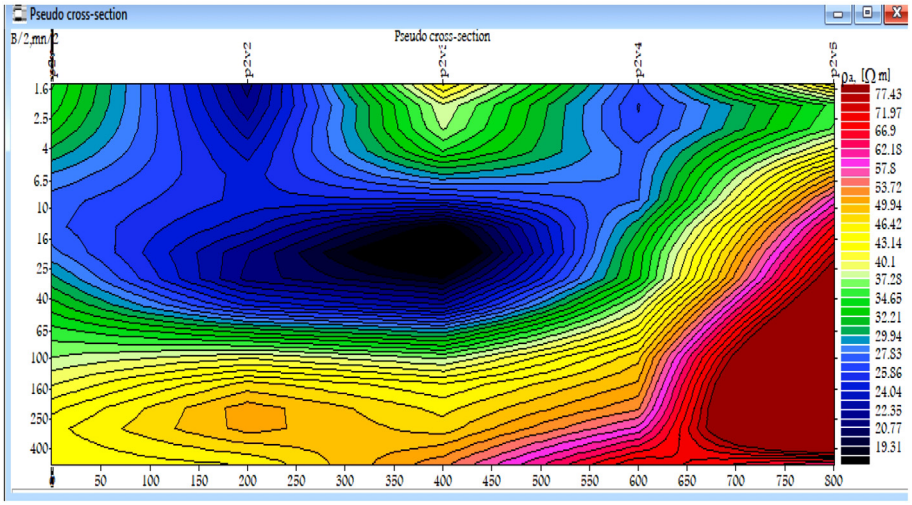

Figure 8. Apparent resistivity pseudo cross section for profile Two.

northern region of the segment has moo resistance. From the four VESs, low resistivity is found beneath P4V4, which has resistivity values of less than 30Ωm, and high resistivity was shown at greater than 67Ωm.

4.1.9. Curve interpretation along with profile five

The results observed from Figure 13 for the VES points of profile five (VES1, VES2, VES3, VES4, and VES5) gave a four-layer model of resistivity. The VES on profile five of P5V1 contains four litho-logic formations and its curve was represented $\rho_1 > \rho_2 > \rho_3 < \rho_4 > \rho_5$ as which was QK-type P5V2 curve represented $\rho_1 > \rho_2 < \rho_3 < \rho_4 > \rho_5$, which was an HK-type curve, and the curve had four layers. The P5V3 curve has five layers and represented $\rho_1 < \rho_2 < \rho_3 > \rho_4 > \rho_5$ which was an AQ-type curve. The P5V4 curve has five layers and its curve represents $\rho_1 < \rho_2 < \rho_3 > \rho_4 < \rho_5$. This kind of layer was an AH-type layer.

4.1.10. Pseudo cross-section along with profile five

Figure 14 represents the pseudo depth section, constructed for P5V1, P5V2, P5V3, P5V4, and P5V5 lining on the survey line oriented from southwest to northeast. Accordingly, there is both lateral and vertical variation in resistivity, with high resistivity at the southern part of the layer for all VESs and the central and middle parts starting from the VESs point of P5V3, but lower resistivity is found in the northern part and southwest region of the section.

4.2. GIS for groundwater potential modelling

Essential components for predicting groundwater potential modeling were used in the study. In this model, six thematic factors: lineament density, lithology, aquifer resistivity, altitude, slope steepness, and drainage density were used. Overlay analysis of multi-criterion evaluation techniques was carried out to find the convincing theme with the help of assigned rank/rate to the individual class of the proposed layers, and then next, the weight of individual characteristics was given to account for their impact on the model. All weighted thematic maps were integrated and combined in QGIS/ArcGIS software based on their impact on groundwater formation. The assigned rank/rate and weight for each theme are shown in Table 2.

4.2.1. Factor data development

The identified thematic layers for producing groundwater potential in the Weserbi Guto catchment were discussed as follows.

4.2.1.1. Slope factor. The steepest slope is vulnerable to higher runoff and may decrease the amount of infiltration. As a result, the small infiltration indicates that groundwater is unlikely to occur over the site. Due to the slow surface runoff, the time for rainwater to penetrate the subsurface is longer. This indicates, that infiltration is inversely proportional to the slope, and so a gentle slope promotes significant groundwater infiltration (H Y et al., 2015). Similarly, Agarwal et al. (2013) preferred that the low-value class be assigned a high rank because the terrain is almost flat, and the maximum value class be classified as a low rank because of the relatively high runoff. The highest slope and lowest rank of the study are 41.7°–52.1° (Table 2), and the northern part along the main river is the low slope (0–10.4°) (Figure 15a). This level incline region falls into the exceptionally high category of groundwater capacity.

4.2.1.2. Topographic factor. The factor varies from 2584 to 3075 m above sea level as per the 12.5m resolution DEM. The topography of the study area is flat, gently sloping, and steeply topped with relatively small cut stream channels. Several drainages in the study area flow from the highland of the Entoto mountain and pass through the flat, undulating topography of the Weserbi Guto plain land. Accordingly, there is infiltration and permeability in the low altitude value, which means that there is a high possibility of finding groundwater (Figure 15b).

4.2.1.3. Lineament density factor. According to Magesh et al. (2012), lineation originated to talk about fault and fractured zones that drive auxiliary porosity and expanded penetrability. Likewise, Kumar et al. (2007) said the availability of lineament area may show permeability zones that indicate groundwater position. This variable is of incredible hydrogeological significance as it gives a course for groundwater development. Since the nearness of lineament, as a rule, demonstrates a saturation zone, the lineament thickness of the zone can be the way to find groundwater potential. It is extremely difficult to close the lineament district (Murasingh, 2014). So in the study, regions with high density (4.8–6km^2) are reasonable for groundwater potential zones (Figure 15c). Generally, lineament plays a vital part in the revival of problematic shake of groundwater and is assigned favorable weight concerning the model.

4.2.1.4. Drainage density factor. Drainage is one of the highest sensitivity factors that play a significant part in the demarcation of groundwater potential zones. They reflect the extent of osmotic precipitation related to outward runoff. For highly permeable rocks in the study area, the penetration into groundwater is high, and less water is transported to the river than the surface water. However, if the rock infiltration rate in the study area is low, there will be little infiltration and more surface water runoff. Therefore, moo water thickness comes about from high energy and high groundwater potential. Drainage densities are high on plateaus and steep slopes and very low on a lift basis. Seepage thickness is characterized as the vicinity of the removal between waterway channels.

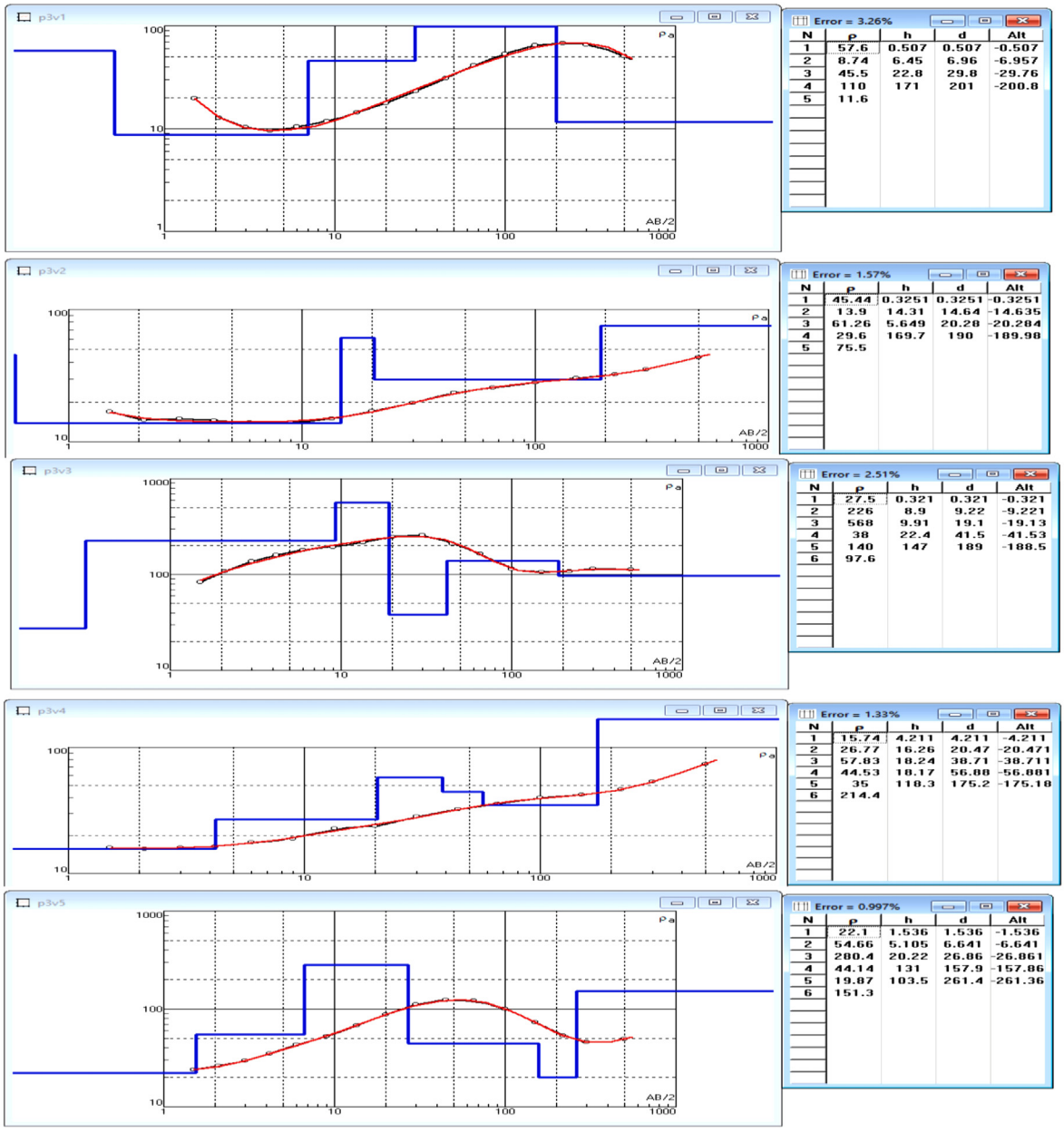

Figure 9. Resistivity sounding curves for Profile Three.

Typically, a degree of the full length of the stream section for all orders per unit zone. Water density is the inverse function of permeability. Fewer penetrable rocks have moo precipitation penetration and, then again, tend to concentrate on surface runoff (Magesh et al., 2012). Higher seepage thickness values are advantageous to runoff and, in this way, show zones with moo groundwater potential (Jesiya and Gopinath, 2020). Zones with moo seepage thickness are relegated to tall positions and bad habits, and vice versa. Accordingly, the drainage density value of the study with 0–1.8km^2 indicates the availability of groundwater was between 7.3 and 9.1km^2 and has low groundwater potential (Table 2; Figure 15d).

4.2.1.5. Aquifer resistivity factor. A small resistance value indicates a hydrous layer (Venkateswaran et al., 2014). The Aquifer resistivity of the Weserbi Guto catchment is mentioned in the Resistivity graph of Profile1up to Profile5 within five VES along with each profile. The highest aquifer resistivity value from those interpretations was 11948.3Ωm and the lowest aquifer resistivity value from the study area was 0.403 Ωm so the aquifer resistivity of the Weserbi Guto Village was found between the above points (Figure 15e).

4.2.1.6. Lithology factor. Lithology may indicate the incidence, movement, and storage of groundwater (A L et al., 2020) and determine the type of porosity and permeability. Porosity decides the amount of water that can be put away, and porousness decides the ease with which water can be pulled back for utilization. The dominant porosity that exists in unconsolidated sediments is inter-granular, with fracture porosity in consolidated rocks and double porosity in some consolidated volcanic and sedimentary rocks. This factor is one of the high-sensitivity variables that influence the availability of groundwater potential within the study area. The lithology of the study was prepared from the aquifer resistivity of geophysical investigation of VES data (Figure 15f). According to Sudhakar et al. (2018), a resistivity range of 0–15 Ohm-m represents the clay layer; a range of 15–25 Ohm-m represents weathered stone, and a range of 25 to 35-ohm-m speaks to semi-weathered to broken stone. They extend from 35 to 120 Ω-m, which speaks to the broken rock, and

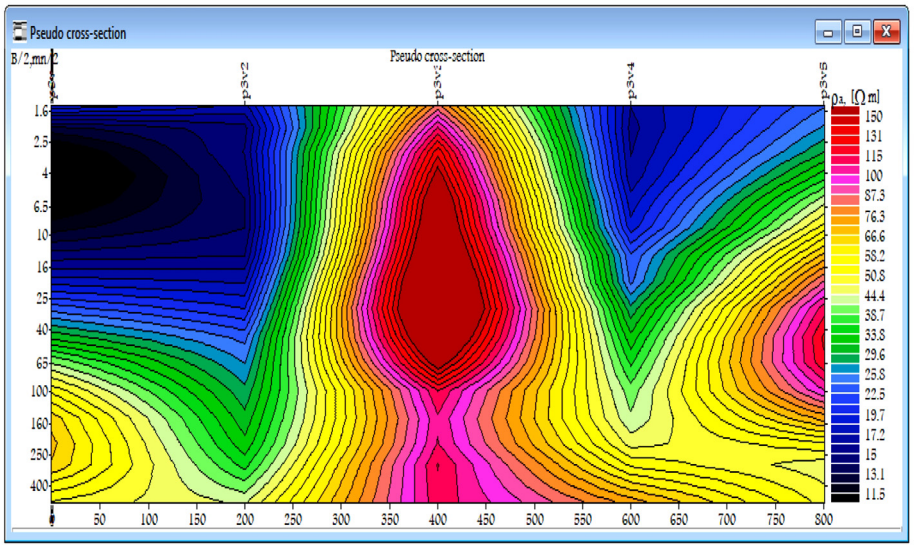

Figure 10. Apparent resistivity pseudo cross section for profile 3.

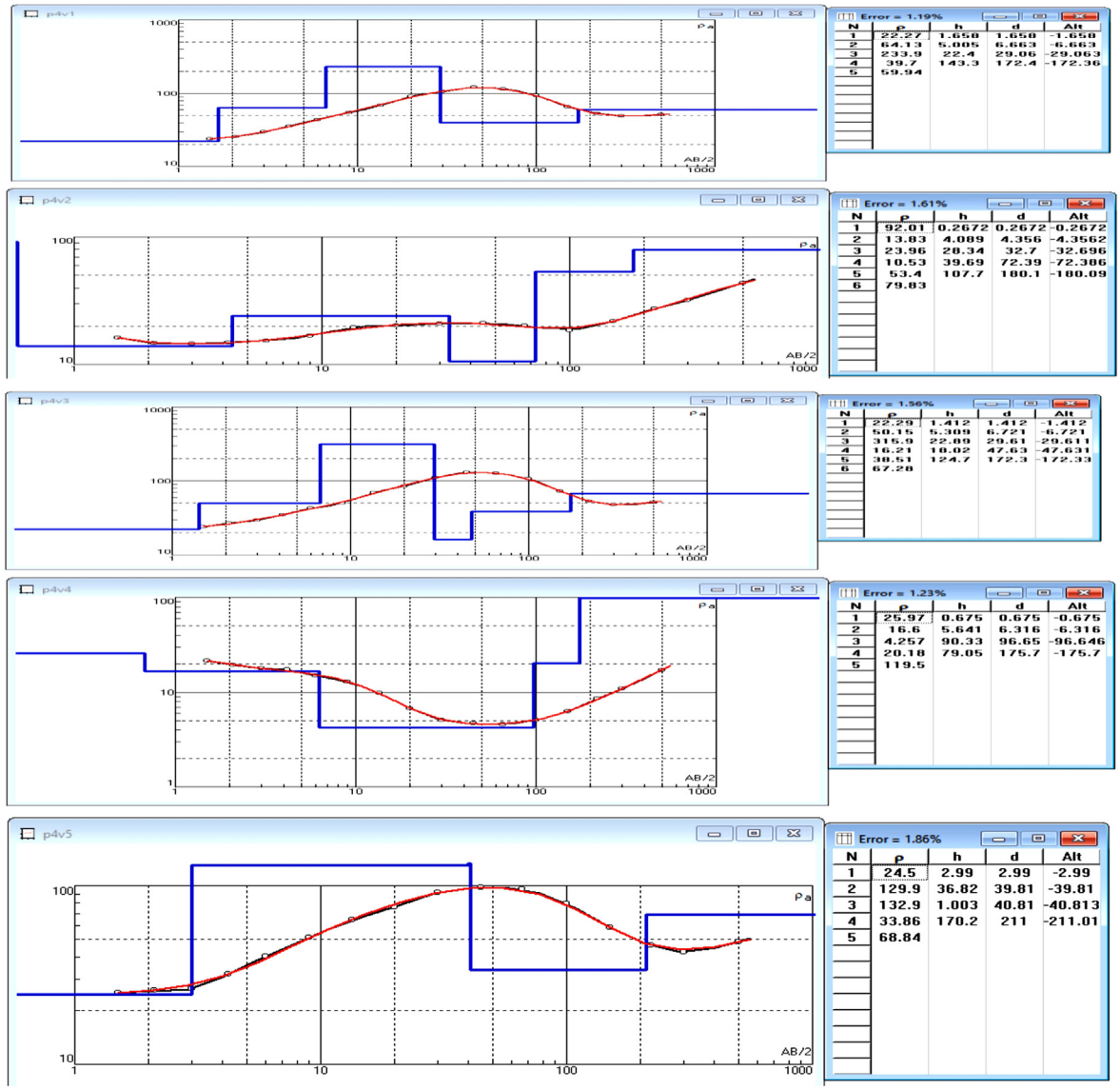

Figure 11. Resistivity sounding curves for Profile Four.

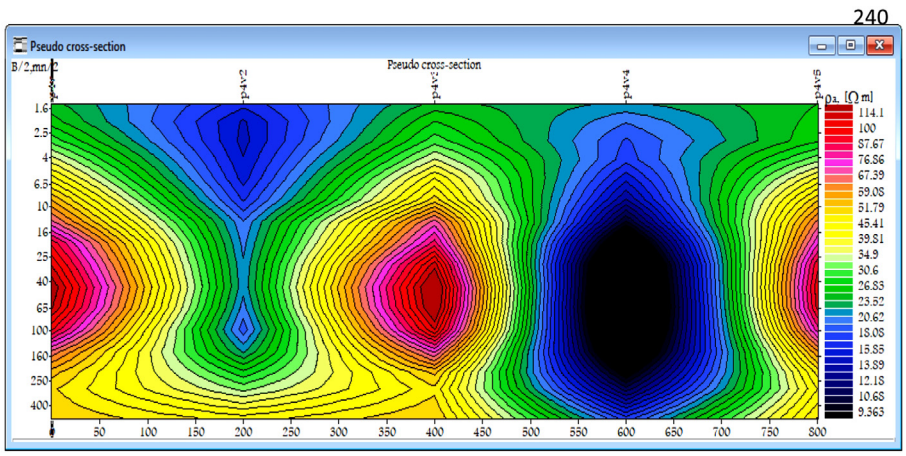

Figure 12. Apparent resistivity pseudo cross section for profile 4.

resistivities over 150 Ω-m speak to the difficult rock that shapes the bedrock. The range from 35-ohm meters to 120-ohm meters represents broken granite, and resistivities above 150-ohm meters represent the hard granite that forms the bedrock.

4.2.2. Groundwater potential model (GPM)

In this portion, GIS techniques were implemented by utilizing weighted overlay innovation to infer an appropriate groundwater potential zone for this investigation. To decide the groundwater potential for a specific zone, increase each scale esteem of the recently classified layer (parameter) by its weight (or rate of effect). The coming cell values are summed up to form the ultimate yield raster that speaks to the potential groundwater range. Higher sum values represent a greater potential for groundwater. For a specific region being evaluated, every parameter scales on an evaluation scale consistent with their significance to different training within the layer. The ideals have been allotted in expressions in their noteworthiness to groundwater events. After each parameter is assigned a scale value (the appropriate value), that mile is weighted. Weight values, from one to the hundredth percent, particularly the relative centrality of the parameters concerning each distinctive groundwater event. The system of the Groundwater Potential Model (GPM) becomes proven in Eq. (1).

$$\begin{aligned} GPM = {} & (DrainageDensity)s * (DrainageDensity)w \\ & + (Topography)s * (Topography)w \\ & + (Aquifer\ Resistivity)s * (Aquifer\ Resistivity)w \\ & + (Slope)s * (Solpe)w + (Lithology)s * (Lithology)w \\ & + (LineamentDensity)s*(Lineament\ Density)w \end{aligned} \tag{1}$$

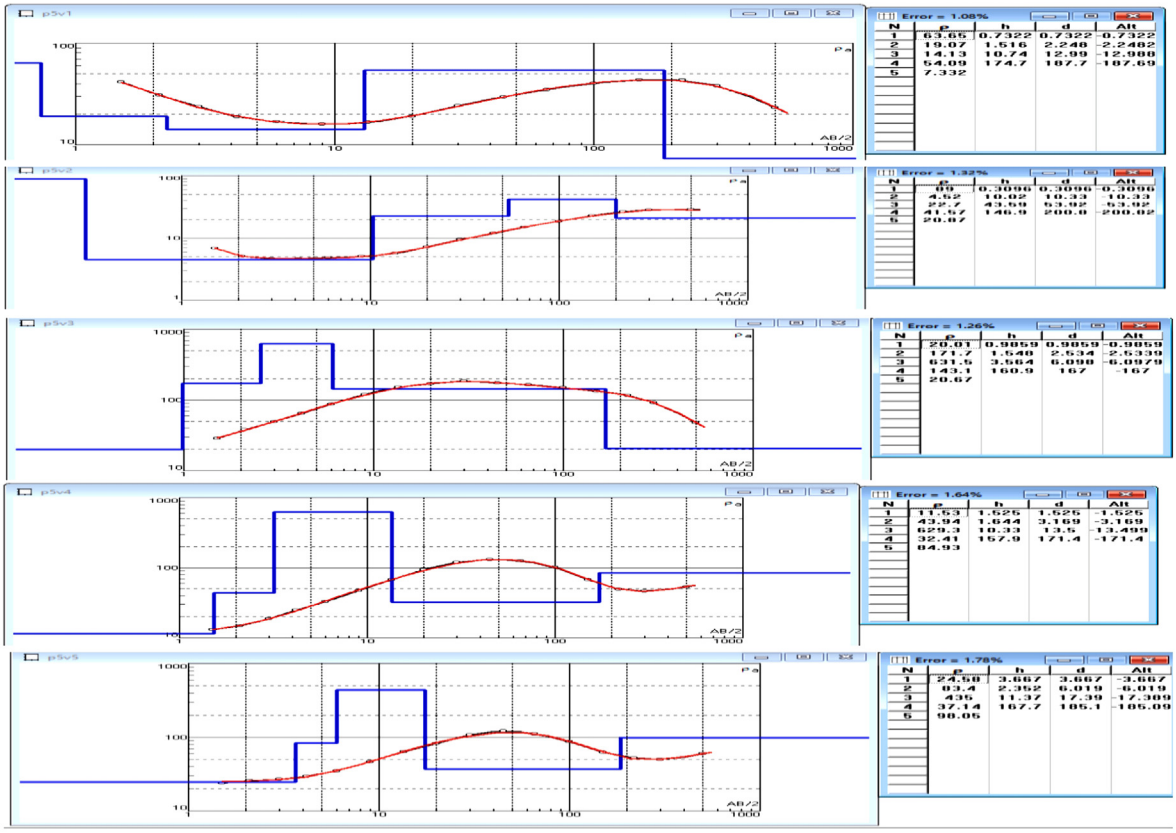

Figure 13. Resistivity sounding curves for Profile five.

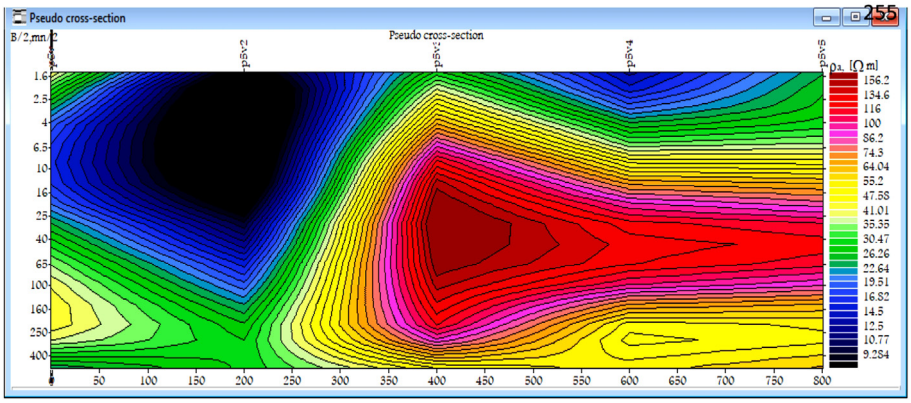

Figure 14. Apparent resistivity pseudo cross section for profile 5.

where w means weighting of the coefficient (1–100%) and s is the scale value (1–5) of the evaluated region. This formula was modeled from (Hammouri et al., 2012), which was used for groundwater exploration through the integration of remote sensing and GIS technology. The groundwater potential outline (Figure 14) appears to indicate that great groundwater potential zones are focused within the central, northeastern, and northwestern parts of the thought zone due to the delicate inclines with moo waste thickness and high penetration capacity. The most appropriate area in the center of the study area was identified due to its low slope class and low drainage density. The map showed that very low-density lineament areas were identified as moderately promising zones, and soak slants and tall waste densities were classified as low-density regions such as auxiliary slopes. This groundwater potential zoning zone was set up within the SE, SW, and northern portions of the considered range. In the study, generally, the reason for high groundwater potential is an area that has low drainage density, low slope, very high lineament density, and low aquifer resistivity of vertical electrical sounding data. The reasons for the low groundwater potential are the very high drainage density, very high gradient, low lineament density, and topographical hill elevation classes shown in Figure 16. Approximately 14.01% of the total area is classified in the "low" zone, 35.85% is classified in the "medium" zone, and 50.14% of the total area is divided into the "tall" zone (Table 3).

Table 2. Final ranking or scale value and Final weightage value for each class.

Factors	Class	Groundwater prospects	Rate	Influence weight (%)
Lithology	clay soil	Very Low	1	10
	silty clay soil	Low	2	
	compacted reddish-brown clay soil	Moderate	3	
	highly weathered and fractured Ignimbrite, trachyte or rhyolite,	High	4	
	highly weathered, fractured, and decomposed Ignimbrite, trachyte, or rhyolite	Very high	5	
Drainage Density (km^2)	0–1.8	Very high	5	22
	1.8–3.6	High	4	
	3.6–5.4	Moderate	3	
	5.4–7.3	Low	2	
	7.3–9.1	Very low	1	
Lineament Density (km^2)	0–1.2	Very low	1	18
	1.2–2.4	Low	2	
	2.4–3.6	Moderate	3	
	3.6–4.8	High	4	
	4.8–6	Very high	5	
Slope gradient (degree)	0–10.4	Very high	5	21
	10.4–20.8	High	4	
	20.8–31.2	Moderate	3	
	31.2–41.7	Low	2	
	41.7–52.1	Very low	1	
Topography/Elevation	2584–2682.2	Very high	5	19
	2682.2001–2780.4	High	4	
	2780.400001–2878.6	Moderate	3	
	2878.600001–2976.8	Low	2	
	2976.800001–3075	Very low	1	
Aquifer Resistivity(ohm-meter)	8.4–50.7	Very high	5	10
	50.7–93.1	High	4	
	93.1–135.4	Moderate	3	
	135.4–177.7	Low	2	
	177.7–220.1	Very low	1	

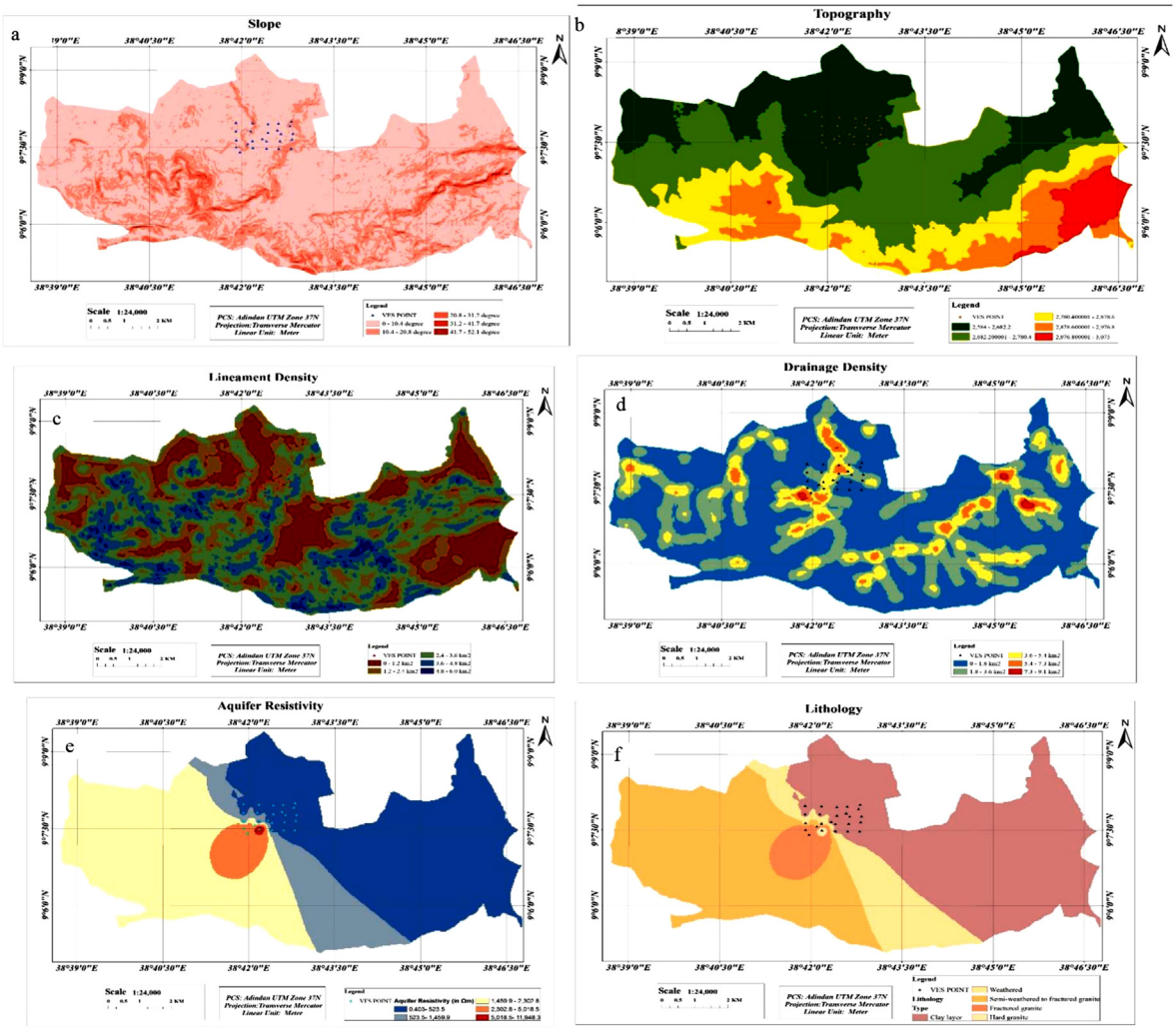

Figure 15. Map of thematic factors.

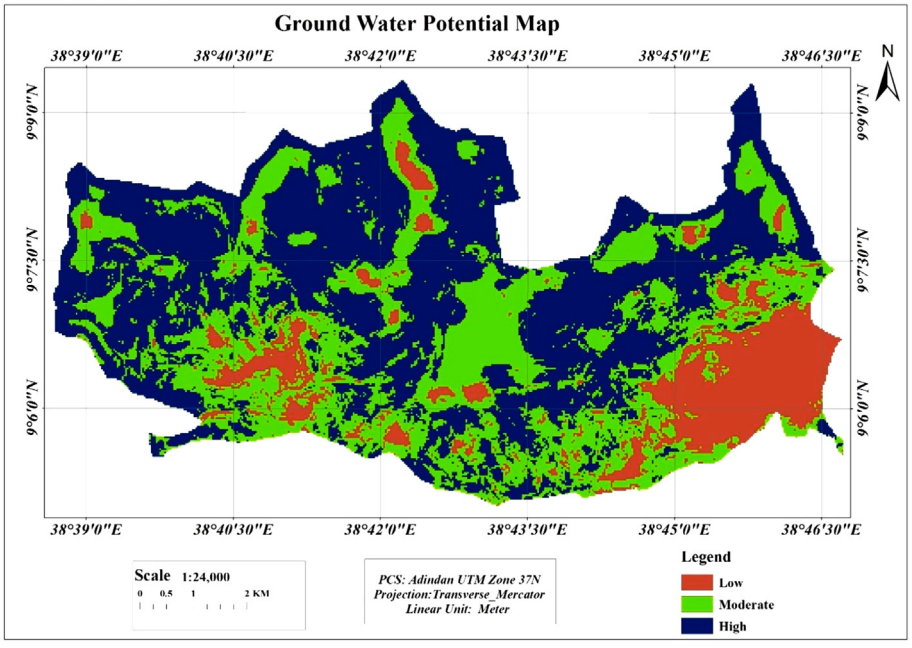

Figure 16. Predicted Groundwater potential zone of the study area.

Table 3. Region in rate and hectares of groundwater potential zonation outline.

S. No	Groundwater Potential Index Zonation(GPIZ)	Area in hectares (ha)	Area in (%)
1	High (369.83–460)	3668.99	50.14
2	Moderate (333.16–369.83)	2623.72	35.85
3	Low (243–333.16)	1024.95	14.01
Total		**7317.66**	**100%**

Table 4. Statistical sum mary of rating.

Parameters	Minimum	Maximum	Mean	Standard deviation
Aquifer Resistivity	1	5	1.99	0.13
Altitude	1	5	3.78	1.15
Drainage density	1	5	4.63	0.70
Lithology	1	5	4.01	0.13
Lineament density	1	5	2.07	1.09
Slope steepness	1	5	4.66	0.58

Table 5. Map removal-based sensitivity analysis.

No.	Parameters removed	Variation index in percent			
		Minimum	Maximum	Mean	Standard deviation
1	ALinTLithDS				
2	LinTLithDS	0	2	1.94	0.23
3	TLithDS	0	6	3.41	1.17
4	LithDS	0	10	4.02	2.09
5	DS	0	17	9.14	2.78
6	S	0	26	9.43	3.53

A = Aquifer resistivity; Lin = Lineament density; T = Topography; Lith = Lithology; D = Drainage density; S=Slope steepness.

4.2.3. Sensitivity Analysis(SA)

As preferred in Thapa et al. (2018), "SA measures the ambiguity or distinction in the output results completed from pragmatic models." Although, SA tells how much each causative map and the weights and the ranks/rates given for their effect on the output map. For identifying the important influential factors in single parameter and map removal SA, single parameter and map removal SA are highly preferred (Thapa et al. (2018); Berhanu & Hatiye (2020)). Accordingly, map removal-based SA was conducted to test the sensitivity of the various thematics used for GPM (Table 4). The mathematical formula for map removal SA is as follows: Eq. (2).

$$SA = \left| \frac{\frac{GPM}{X} - \frac{GPM'}{X'}}{GPM} \right| * 100\% \quad (2)$$

where GPM and GPM′ are the output of the groundwater potential model index of all the thematic factors and when one of the thematic factors is removed, respectively. X is the number of the full thematic factors used to compute GPM, and X′ is the number of thematic factors used to compute GMP'.

In multiple map removal sensitivity analysis, parameters causing the least variation based on the mean statistical value that was computed in QGIS (Table 4) on the final output were removed first, followed by the second least, and so on. The sensitivity index shows that slope steepness is a highly influential factor of GPM while aquifer resistivity is the least influential factor (Table 5).

4.2.4. Validation of the model

A total of 11 existing groundwater point data sets, including springs, deep wells, hand-dug wells, and on-site monitoring, were used for validating the model. The station's minimum and maximum discharging yields are 0.2 l/s and 20 l/s, respectively. The groundwater potential index was overlaid with the collected groundwater inventory data, and the index was validated with the amount of discharging yield in liters per second (Figure 17). As a result, 18.2% of the stations fell into the low (243–333.16) GPIZ, while 54.5% and 27.3% of the stations fell into the moderate (333.16–369.83) and high (369.83–460) zones, respectively. The moderate classes were aligned within the highest amount of discharging yield (20 l/s) at a large depth (461 m) across the study area. Even the lowest yield (0.3 l/s) was found in this zone (Figure 17).

5. Conclusion

The main objective of this paper is to use a Geographical Information System and geophysical survey through VES techniques for the assessment and investigation of the spatial dissemination of groundwater

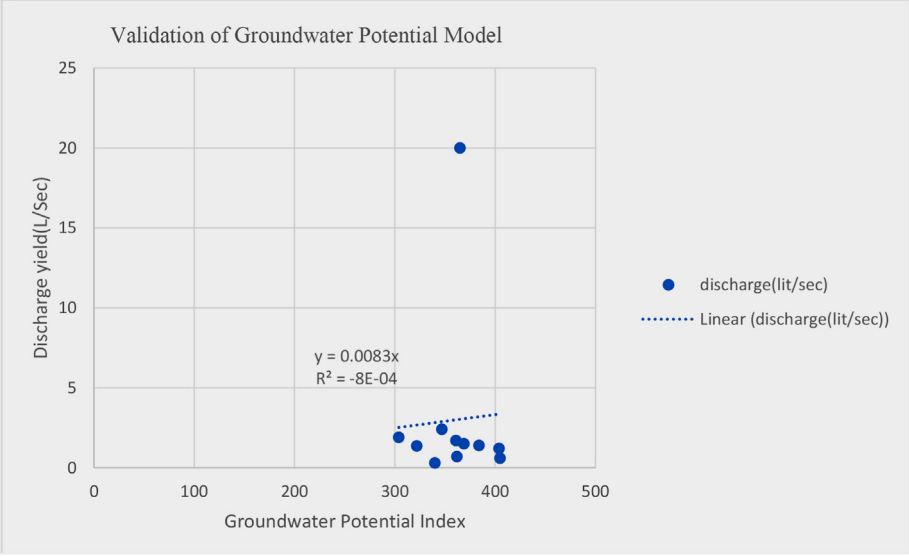

Figure 17. Graphs of result validation.

potential zones in a zone of about 7317.66 ha. GIS innovation employs a weighted direct combination strategy to outline a region's groundwater potential zone based on groundwater persuasive components. In this research, six parameters have been selected. These substantial constraints for the region of the groundwater potential outline are the resistivity curves for each VES data like aquifer resistivity, topography, slope steepness, drainage density, and lithology and lineament density. They have more effects on the occurrence of groundwater potential maps before overlay analysis by assigning the rating scales and percentage weights; it is possible to define important criteria that have a greater impact on results than other criteria. In the VES point curve and cross-section along all profiles data were generated to give the value of soil thickness and depth, as well as lithology sections of the area, which were interpreted based on the aquifer resistivity value. Based on the geo-electrical results, the low resistivity anomalies show the chance of groundwater availability and are assigned as high groundwater zones. This lowest resistivity is probably due to alluvial deposits and clayey soils. However, the highest resistivity anomalies show less occurrence of water, so the availability of groundwater is low because there may be high drainage density and low permeability with high runoff. The highest resistivity anomalies may be formed due to sand soils and rocks. The geoelectric segment sideway of Profile 1 of the third geoelectric coat ranges from 40 ohmm to 76 ohmm and has an average thickness of 128.2 m to an average depth of 156.67 m, which is considered highly cracked basalt. This area is a relatively conductive area for groundwater exploration potential, with a large thickness and a maximum depth of 233m. The second profile of the fourth geo-electric layer has a resistivity value ranging from 35 Ω to 54 Ω, which was highly fractured basalt. This area is a conductive area for groundwater potential with a large thickness and a maximum depth of 226m. The geoelectric section along Profile 3 of the third geoelectric layer has a resistivity value in the range of 30ohmm to 57ohmm, with an average thickness of 42.5m and an average depth of 64.96m, which was interpreted as a highly fractured basalt, which was saturated zone and confined for groundwater potential at a maximum depth of 175.2m. In the geo-electric section along with profile four, the fourth layer possesses an apparent resistivity and thickness value of 33 ohm–54 ohmm and 136.5 m at an average depth of 184 m, which could be the response of highly fractured basalt and saturated with groundwater potential at a maximum depth of 211 m. In the geo-electric section, along with profile five, the tertiary geoelectric coat has a lower resistance value within the array of 32 Ω to 54-ohm meters at an average thickness of 161.8 m and an average depth of 186.25 m, which was highly fractured basalt. This layer has low resistivity at its maximum depth. The area was a conductive area for groundwater potential with a very large thickness and a maximum depth of 200m. The boundary zone of the groundwater potential outline is separated into three zones: low, medium, and high. The low zone demonstrates that low is suitable for groundwater investigation.

On the other hand, the high zone appears to be the leading range for groundwater investigation. There are areas of high groundwater potential in the north, northeast, and northwest, corresponding to very low and low slopes, respectively, due to the resistivity of the aquifer and the high conduction density of the study area. Low groundwater potential falls in the area with very high and high aquifer resistivity, high slope steepness, and high drainage density. Satisfactory results were gotten by comparing well abdicate information with the groundwater potential zone outline of the thought zone. The low drainage areas were the points for the confined groundwater saturation zone, which was correlated to the resistivity found in profiles; Profile 1 (P1V4), Profile 4 (P4V2), and Profile 5 (P5V2). So, the possible aquifer zones were thought to be highly fractured and weathered basalt.

Code availability section

Hardware requirements: computer, handheld GPS, Syscal Junior Switch 72 (IRIS).

Software required:
Ip2Win (http://geophys.geol.msu.ru/demo_exe/SetUp_lt.exe).
QGIS (https://qgis.org/en/site/forusers/download.html#).

Declarations

Author contribution statement

Mr. Desalegn Dhinsa: Conceived and designed the experiments; Contributed reagents, materials, analysis tools or data; Wrote the paper

Dr. Fekadu Tamiru: Performed the experiments; Contributed reagents, materials, analysis tools or data.

Mr. Birhanu Tadesa Edosa: Analyzed and interpreted the data; Contributed reagents, materials, analysis tools or data; Wrote the paper.

Funding statement

This research did not receive any specific grant from funding agencies in the public, commercial, or not-for-profit sectors.

Data availability statement

Data associated with this study has been deposited at http://10.13.8.73:8080/wurepository/

Declaration of interest's statement

The authors declare no conflict of interest.

Additional information

No additional information is available for this paper.

Acknowledgements

We would like to give thanks to our God before anything, who gives us full health, peace, knowledge, and wisdom to accomplish this work. We extend our thanks to Wollega University for helping us to provide materials and instrument support for this research.

References

Agarwal, E., Agarwal, R., D.Garg, R., Garg, P., 2013. Delineation of groundwater potential zone: an AHP/ANP approach. Earth Syst. Sci. 887–898.

AL, A., Thomas, J., Reghunath, R., 2020. Multi-criteria Decision Analysis for Delineation of Groundwater Potential Zones in a Tropical River basin Using Remote Sensing, GIS, and Analytical Hierarchy Process (AHP). Groundwater for Sustainable Development 1–18.

Berhanu, K.G., Hatiye, S.D., 2020. Identification of groundwater potential zones using proxy data: case study of megech watershed, Ethiopia. J. Hydrol.: Reg. Stud. 1–20.

Çelik, R., 2019. Evaluation of groundwater potential by GIS-based multicriteria decision making as a spatial prediction tool: case study in the tigris river batman-hasankeyf sub-basin, Turkey. Water 1–16.

Hammouri, N., El-Naqa, A., Barakat, M., 2012. An integrated approach to groundwater exploration using remote sensing and geographic information system. J. Water Resour. Protect. 717–724.

HY., A., Priju, C.P., Prasad, N., 2015. Delineation of groundwater potential zones in deep midland aquifers along bharathapuzha river basin, Kerala using geophysical methods. Aquatic Procedia 1039, 1046.

Jesiya, N., Gopinath, G., 2020. A Fuzzy-Based MCDM–GIS Framework to Evaluate Groundwater Potential index for Sustainable Groundwater Management - A Case Study in an Urban-Periurban Ensemble, Southern India. Groundwater for Sustainable Development 1–37.

Jiaca, 2002. Groundwater Development and Water Supply Training Project. http://www.Jica.go.jp.

Kumar, P.K., Gopinath, G., Seralathan, P., 2007. Application of remote sensing and GIS for the demarcation of groundwater Kerala, southwest coast of India. International Journal of Remote Sensing potential zones of a river basin in 5583–5601.

Magesh, N., Chandrasekar, N., Soundranayagam, J.P., 2012. Delineation of groundwater potential zones in Theni district, Tamil Nadu, using remote sensing, GIS, and MIF techniques. Geosci. Front. 189–196.

Murasingh, S., 2014. Analysis of groundwater potential zones using electrical resistivity, RS & GIS Techniques in a Typical Mine Area of Odisha. Rourkela National Institute of Technology 1–74.

Sudhakar. A Ramakrishna, C., Saxena, P.R., 2018. Electrical resistivity survey for groundwater investigations and evaluation of the granite –basalt formation around narayankher, medak district, telangana state, India. International Journal of Trend in Research and Development 10–15.

Thapa, R., Gupta, S., Guin, S., Kaur, H., 2018. Sensitivity analysis and mapping the potential groundwater vulnerability zones in Birbhum district, India: a comparative approach between vulnerability models. Water Science 44–66.

Venkateswaran., S., Prabhu, M., Karuppannan., S., 2014. Delineation of groundwater potential zones using geophysical and GIS techniques in the sarabanga Sub basin, cauvery river, Tamil nadu, India. International Journal of Current Research and Academic Review 58–75.